

# New Type of Ion-Sensitive Field-Effect Transistor with Sensing Region Separate from Gate-Controlled Region

Ryongbin Lee<sup>1</sup>, Dae Woong Kwon<sup>1</sup>, Sihyun Kim<sup>1</sup>, Hyun-Sun Mo<sup>2</sup>,  
Dae Hwan Kim<sup>2</sup>, and Byung-Gook Park<sup>1,\*</sup>

<sup>1</sup>Inter-University Semiconductor Research Center (ISRC) and Department of Electrical and Computer Engineering,  
Seoul National University, Seoul 151-742, Republic of Korea

<sup>2</sup>School of Electrical Engineering, Kookmin University, Seoul 136-702, Republic of Korea

A new type of ISFET is proposed where the proposed ISFET channel is divided into a gate-controlled region (Region<sub>gate</sub>) and sensing region (Region<sub>sense</sub>). The ISFET is operated by controlling the gate voltage of the Region<sub>gate</sub> with the attached biomolecules on the gate dielectric of the Region<sub>sense</sub>. When the gate voltage is applied over the threshold voltage ( $V_{th}$ ), the channel resistance of the Region<sub>gate</sub> sharply decreases and the larger channel resistance of the Region<sub>sense</sub> limits the ISFET current. Thus, the on-current ( $I_{on}$ ) of the ISFET is controlled by the attached biomolecule charge on the gate dielectric of the Region<sub>sense</sub>. Our proposed ISFET has many advantages over conventional ISFETs. From TCAD simulations, the proposed ISFET was found to have higher sensitivity according to pH levels than conventional ISFETs due to the unique limitation of the  $I_{on}$  by the channel resistance change of the Region<sub>sense</sub>. Additionally, the field-dependent drift effect can be mitigated, because hydrogen ions or biomolecules in the solution are hardly affected by the gate voltage. Furthermore, the proposed ISFET has uniform  $I_{on}$  change regardless of  $V_{th}$  variation, because only the channel resistance of the Region<sub>sense</sub> determines the  $I_{on}$ .

**Keywords:** Field-Effect Transistor (FET) Based Biosensor, Ion-Sensitive Field-Effect Transistor (ISFET), pH Sensor.

## 1. INTRODUCTION

Silicon nanowire (SiNW) based ion-sensitive field effect transistors (ISFET) have attracted attention for biomolecule sensing due to being label-free, being highly sensitive, and having real-time detection.<sup>1–3</sup> In addition, the CMOS-compatible fabrication process of ISFET sensors has shown great potential for mass production due to good uniformity, high reproducibility, and low-cost fabrication.<sup>1–5</sup> However, there are several obstacles that must be overcome in order to commercialize ISFETs successfully as a biosensor. In terms of on-current ( $I_{on}$ ) sensitivity, the maximum threshold voltage ( $V_{th}$ ) shift of ISFET is limited to 60 mV/pH at room temperature due to Nernst limitation,<sup>6</sup> so the  $I_{on}$  change is limited by the  $V_{th}$  shift. To achieve a higher  $I_{on}$  change than that by the  $V_{th}$  shift, a fundamentally different mechanism that induces the  $I_{on}$  change needs to be introduced. Furthermore, the current drift effect in ISFETs<sup>7,8</sup> has prevented stable current sensing since  $I_{on}$  varies with liquid gate bias ( $V_{LG}$ ), pH level

(concentration of hydrogen ions), and measurement time. To solve these problems, a novel ISFET with a sensing region separate from a gate-controlled region is proposed, as shown in Figure 1. The proposed ISFET can have higher  $I_{on}$  sensitivity than conventional ISFETs since the resistance change of the sensing region (Region<sub>sense</sub>) from the binding of target molecules induces  $I_{on}$  change. In addition, the field-enhanced current drift can be mitigated, because the proposed ISFET can detect hydrogen ions or biomolecules in the solution without applying  $V_{LG}$ .

In this study, we rigorously investigate the physical origins of the high  $I_{on}$  sensitivity in the proposed structure by using TCAD simulations.<sup>9</sup> Moreover, the doping condition of the Region<sub>sense</sub> is optimized to maximize the  $I_{on}$  sensitivity.

## 2. SIMULATED DEVICE STRUCTURE AND FABRICATION PROCESS

The device architecture and physical parameters of the proposed ISFET used in this work are shown in Figure 2 and

\*Author to whom correspondence should be addressed.

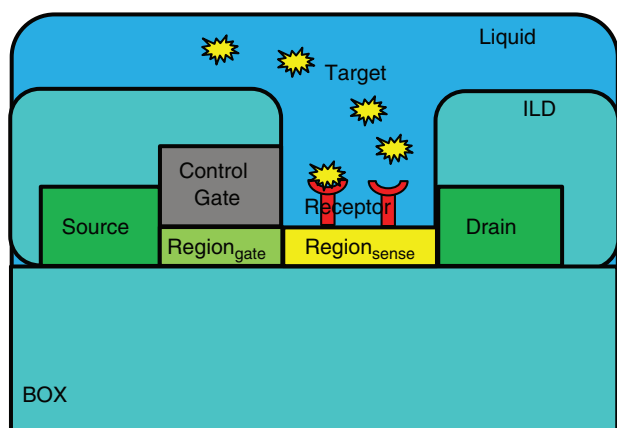


**Figure 1.** A schematic diagram of the newly proposed ISFET.

Table I, respectively. The channel of the proposed ISFET is separated into Region<sub>gate</sub> and Region<sub>sense</sub>. The Region<sub>gate</sub> is doped with boron of  $10^{17} \text{ cm}^{-3}$  and the Region<sub>sense</sub> is doped with phosphorus of  $10^{19} \text{ cm}^{-3}$  to form a high resistance region where the inversion occurs in Region<sub>gate</sub> by increasing the gate voltage of the Region<sub>gate</sub> ( $V_G$ ). Only the Region<sub>sense</sub> is opened to contact the Region<sub>sense</sub> to the solution, including hydrogen ions or biomolecules. The detailed fabrication process for the proposed ISFET is provided in Figure 3. After the 100 nm-thick SOI (Silicon-on-insulator) wafer is prepared, the SOI is doped with boron ( $5 \times 10^{12} \text{ cm}^{-2}$  dose, 20 keV) to form a  $p$ -type channel.

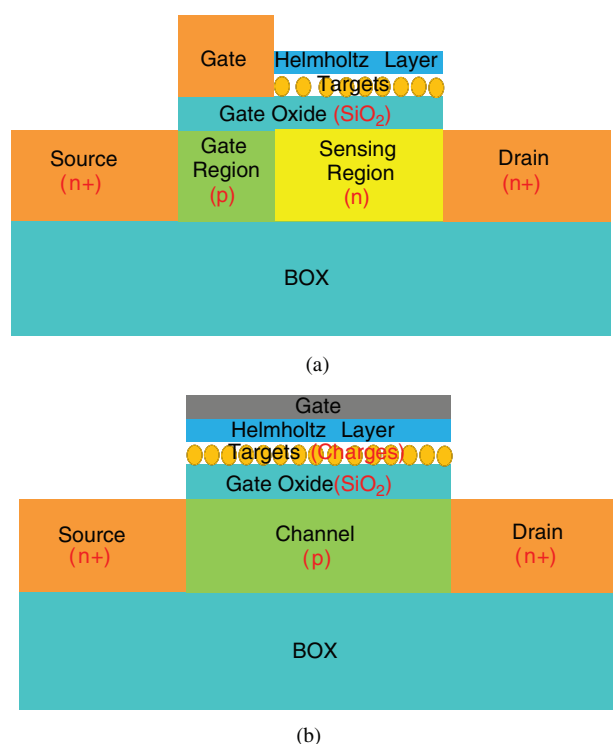


**Figure 2.** Device structures used in the simulations: (a) Proposed ISFET and (b) conventional ISFET.

**Table I.** Device parameters used in these simulations.

Simulation parameters	
Width	$1 \mu\text{m}$
$L_{\text{sense}}$	$1 \mu\text{m}$
$L_{\text{gate}}$	200 nm
$T_{\text{ox}}$	2 nm
$T_{\text{channel}}$	20 nm
$T_{\text{Helmholtz}}$	0.1 nm
$T_{\text{box}}$	100 nm
S/D doping	$1 \times 10^{20} \text{ cm}^{-3}$ (Arsenic)
Region <sub>gate</sub> doping	$1 \times 10^{17} \text{ cm}^{-3}$ (Boron)
Region <sub>sense</sub> doping	$1 \times 10^{19} \text{ cm}^{-3}$ (Phosphorus)

Then, the gate oxide and poly-silicon gate are formed by oxidation and LPCVD, respectively. After dry-etching the gate stack, the source/drain and the gate are simultaneously doped with arsenic ( $3 \times 10^{15} \text{ cm}^{-2}$  dose, 40 keV). To define the Region<sub>sense</sub>, the poly-silicon gate is partially etched, as depicted in Figure 3(c). In addition, the source/drain, the gate, and the Region<sub>sense</sub> are lightly doped with phosphorus ( $1 \times 10^{14} \text{ cm}^{-2}$  dose, 40 keV), as seen in Figure 3(d). Lastly, the conventional back-end process is performed and only the sensing-area above the Region<sub>sense</sub> is opened by the RIE (Reactive-Ion Etching) process in  $\text{CHF}_3/\text{CF}_4$  plasma.<sup>11, 12</sup>

In the simulations, we assumed that the Helmholtz layer can be considered a dielectric layer with a few angstrom thickness.<sup>10</sup> Hydrogen ions or biomolecules attached to the gate oxide of the Region<sub>sense</sub> are modeled as positive or negative charges. The site-binding theory is used to model the sensing mechanism of ions or molecules with charge<sup>8</sup> and all simulations are conducted with the Sentaurus<sup>TM</sup> TCAD simulator from Synopsys Inc.

### 3. RESULTS AND DISCUSSION

Figure 4 shows the equivalent resistance model of the proposed ISFET where two-divided channel regions are modeled as two different resistances (resistance of Region<sub>gate</sub>: $R_c$  and resistance of Region<sub>sense</sub>: $R_s$ ). In the sub-threshold region, the  $R_c$  is much larger than the  $R_s$  since the channel is not completely formed in the Region<sub>gate</sub>. Thus, the device current is modulated as a function of the  $V_G$ , similar to conventional MOSFETs. However, the  $R_s$  becomes larger than the  $R_c$  in the saturation region where the channel inversion occurs in the Region<sub>gate</sub> by increasing the  $V_G$  while the  $R_c$  decreases sharply as a consequence. As a result, the  $I_{\text{on}}$  of the proposed device is limited by the large  $R_s$  regardless of the  $V_G$ . As expected, Figure 5 confirms that the proposed ISFET current is modulated as a function of the  $V_G$  in the subthreshold region and the current change is negligible regardless of the  $V_G$  in the saturation region. Furthermore, Figure 5 shows the transfer curves of the proposed ISFET in solutions with different pH levels. Interestingly, only the  $I_{\text{on}}$  becomes reduced by the nearly unchanged  $V_{\text{th}}$  as pH levels are

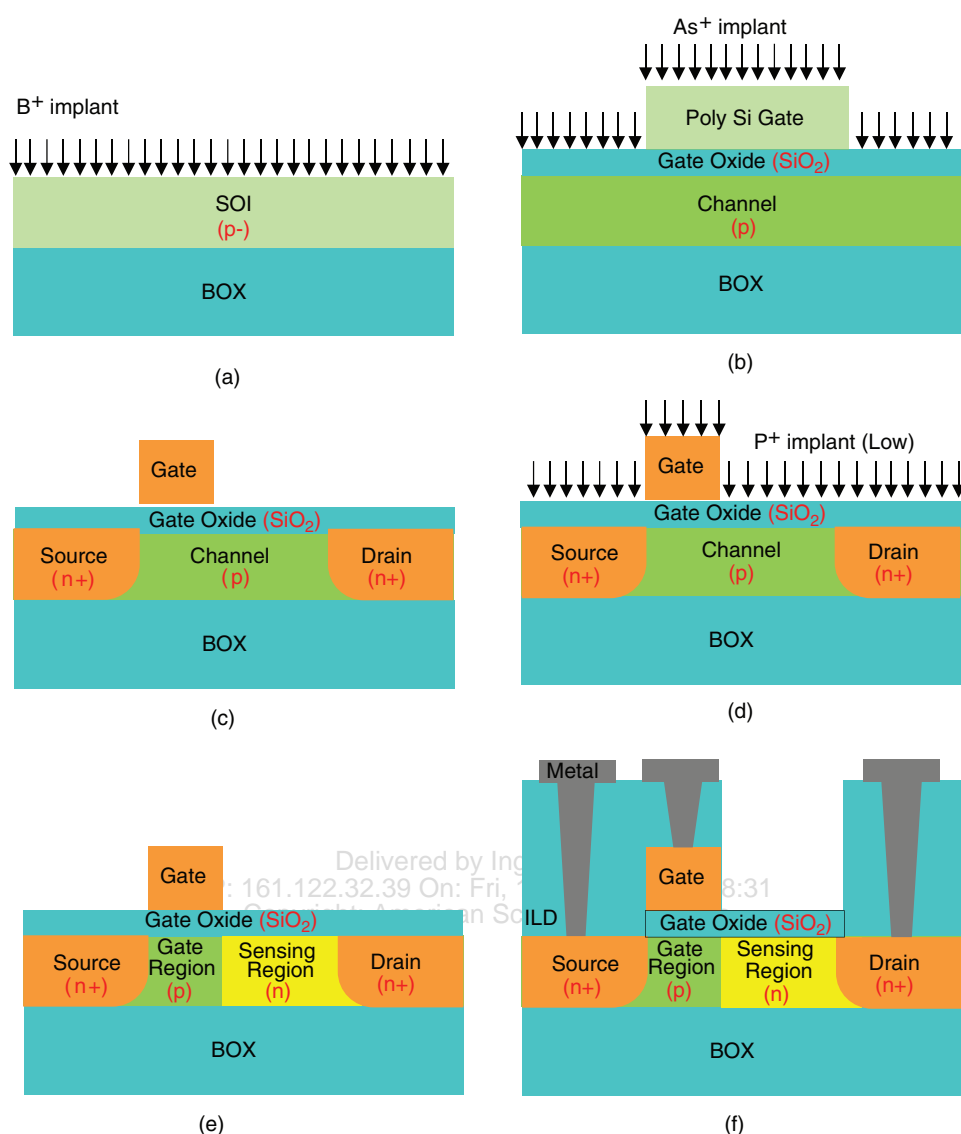


Figure 3. The schematic diagrams of the process flow for the proposed ISFET.

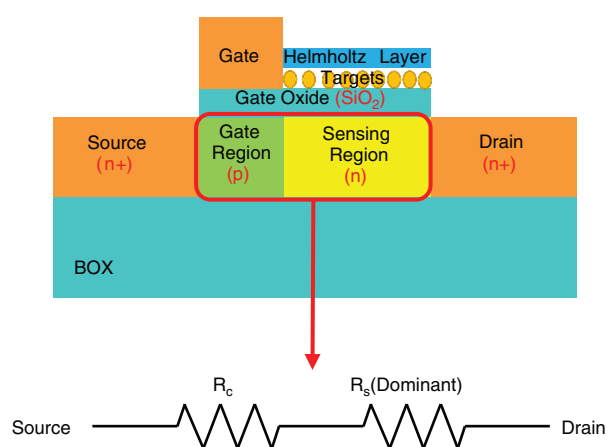


Figure 4. Resistance model of the two separate channel regions (Region<sub>gate</sub> and Region<sub>sense</sub>).

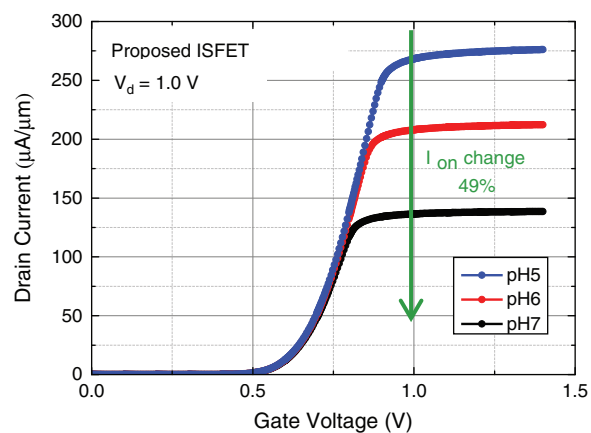
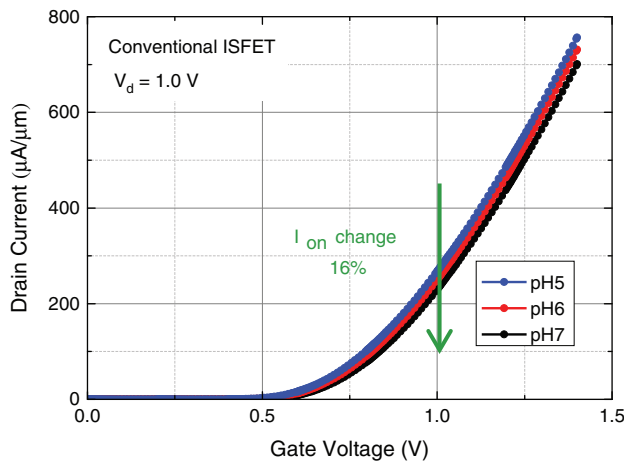


Figure 5. Transfer curves of *n*-type proposed ISFET (pH sensor) according to pH level.



**Figure 6.** Transfer curves of *n*-type conventional ISFET (pH sensor) according to pH level.

increased. The pH level increase means that more negative charges are attached to the Region<sub>sense</sub>. Due to the negative charges bound on the Region<sub>sense</sub>, holes are induced in the *n*-type doped Region<sub>sense</sub> with channel inversion. The holes in the Region<sub>sense</sub> increase the  $R_s$  while the elevated

$R_s$  reduces the  $I_{on}$  of the ISFET since the  $I_{on}$  is determined by the  $R_s$ . It should be noted that more negative charges in the Region<sub>sense</sub> induce more holes so that the  $R_s$  becomes larger. Consequently, the  $I_{on}$  gets reduced at higher pH levels due to the larger  $R_s$  from negative charges attached to the Region<sub>sense</sub>.

In Figures 5 and 6, the sensitivity of the proposed ISFET is compared to that of conventional ISFET. Furthermore, the proposed ISFET has higher sensitivity (represented by  $I_{on}$  change) than conventional ISFET. The  $I_{on}$  change is improved three times, as the change in  $R_s$  is much larger than that in the channel resistance in the conventional ISFET. Moreover, this  $I_{on}$  change is maintained constantly throughout the saturation region in the proposed ISFET while it varies in the conventional ISFET. For the read-out circuit system, the operating voltage of the proposed ISFET can be easily determined since it is not necessary to consider the various sensitivity depending on the gate voltage.

To maximize the sensing performance of the proposed ISFET, the Region<sub>sense</sub> resistance should be raised by lowering the arsenic doping concentration of the Region<sub>sense</sub>. As shown in Figure 7, the  $I_{on}$  change increases when the Region<sub>sense</sub> is doped with  $4 \times 10^{18} \text{ cm}^{-3}$  rather than  $1 \times 10^{19} \text{ cm}^{-3}$ , which is verified in Figure 8. When the same amount of charges ( $N_{ac} = 1.1 \times 10^{13} \text{ cm}^{-2}$ ) are bound

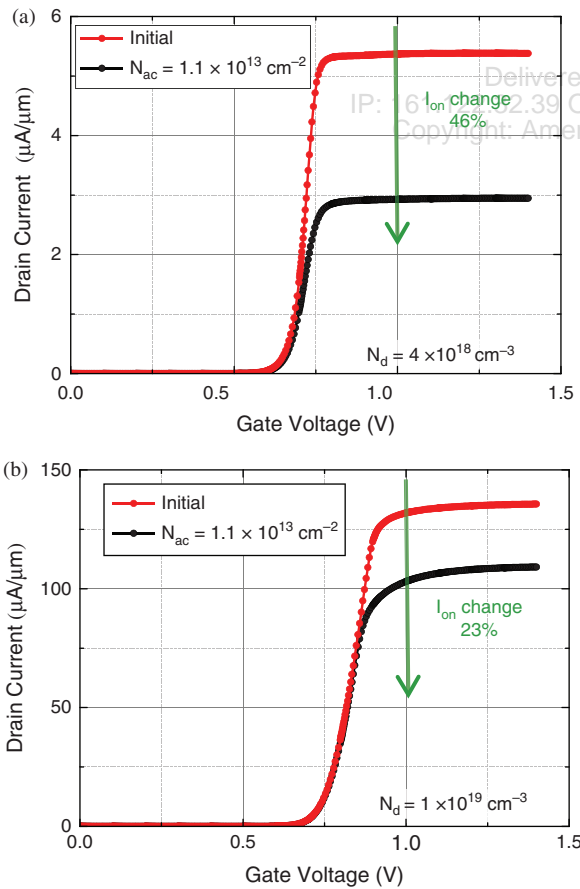


**Figure 7.** Comparison of on-current change due to attached charges ( $N_{ac}$ ) between proposed ISFETs with two different Region<sub>sense</sub> dopings. (a)  $N_d = 4 \times 10^{18} \text{ cm}^{-3}$  and (b)  $N_d = 1 \times 10^{19} \text{ cm}^{-3}$ .

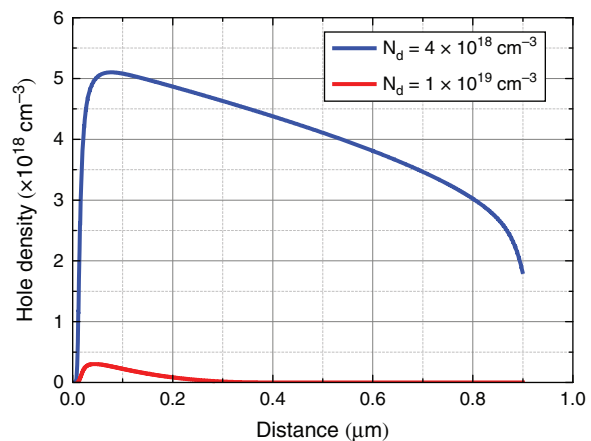
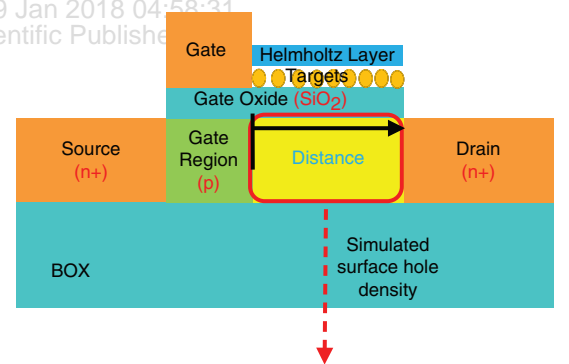


**Figure 8.** Simulated surface hole density in the Region<sub>sense</sub> with two different doping conditions ( $N_{ac} = 1.1 \times 10^{13} \text{ cm}^{-2}$ ).

on the  $\text{Region}_{\text{sense}}$ , the stronger hole inversion occurs in the  $\text{Region}_{\text{sense}}$  with the lower arsenic doping concentration (namely, more holes in the  $\text{Region}_{\text{sense}}$  imply a larger  $R_s$  change). Consequently, it is advantageous to apply the lower doping concentration to the  $\text{Region}_{\text{sense}}$  within the range where a stable signal-to-noise ratio (SNR) can be obtained, because the  $\text{Region}_{\text{sense}}$  with the lower doping concentration reacts sensitively to the attached target charges.

Additionally, the proposed ISFET is free from serious current drift. In previous studies,<sup>6,7</sup> it has been reported that one of the most critical causes of the drift effect in ISFETs results from external  $V_{\text{LG}}$ , which accelerates ion diffusion into the gate oxide of ISFETs. As our proposed device does not have the  $V_{\text{LG}}$  applied to the sensing region, the field-dependent current drift can be alleviated when compared to conventional ISFETs that apply the  $V_{\text{LG}}$ .

#### 4. CONCLUSION

In this work, we proposed a new type of ISFET with the sensing region separate from the gate-controlled region. Through TCAD simulations, the sensing mechanism is analysed rigorously and the pH sensitivity of the proposed ISFET is compared to that of the conventional ISFET. As a result, the  $I_{\text{on}}$  sensitivity of the proposed ISFET surpasses that of the conventional ISFET due to the unique limitation of the  $I_{\text{on}}$  by the channel resistance change of the  $\text{Region}_{\text{sense}}$ . Furthermore, the superior  $I_{\text{on}}$  change of the proposed ISFET is maintained in the entire saturation region, which makes it easier to determine the operation voltage with optimized sensitivity in readout circuit systems. Furthermore, the field-dependent current drift effect can be suppressed because the proposed ISFET does not operate with the  $V_{\text{LG}}$ . Based on these results, the proposed ISFET can be a promising solution for the highly sensitive and stable current sensing of biomolecules.

**Acknowledgments:** This work was supported by the Brain Korea 21 Plus Project in 2017 in part by the National Research Foundation of Korea (NRF) funded by the Korean Government under Grant 2016R1A5A1012966 and 2016R1A6A3A01006588 and in part by the Future Semiconductor Device Technology Development Program (10044842) funded by Ministry of Trade, Industry and Energy (MOTIE) and Korea Semiconductor Research Consortium (KSRC).

#### References and Notes

1. Z. Li, Y. Chen, X. Li, T. I. Kamins, K. Nauka, and R. S. Williams, *Nano Lett.* 4, 245 (2004).
2. N. C. Tansil and G. Zhiqiang, *Nano Today* 1, 28 (2006).
3. M. Curreli, R. Zhang, F. N. Ishikawa, H. K. Chang, R. J. Cote, C. Zhou, and M. E. Thompson, *IEEE Trans. Nanotechnol.* 7, 651 (2008).
4. I. Park, Z. Li, A. P. Pisano, and R. S. Williams, *Nanotechnology* 21, 015501 (2010).
5. E. Stern, J. F. Klemic, D. A. Routenberg, P. N. Wyrembak, D. B. Turner-Evans, A. D. Hamilton, D. A. LaVan, T. M. Fahmy, and M. A. Reed, *Nature* 445, 519 (2007).
6. O. Knopfmacher, A. Trasov, W. Fu, M. Wipf, B. Niesen, M. Calame, and C. Schonberger, *Nano Lett.* 10, 2268 (2011).
7. D. Kwon, J. H. Lee, S. Kim, R. Lee, H. Mo, J. Park, D. H. Kim, and B.-G. Park, *IEEE Electron Device Lett.* 37, 652 (2016).
8. S. Kim, D. W. Kwon, R. Lee, D. H. Kim, and B.-G. Park, *Japanese Journal of Applied Physics* 55, 6S1 (2016).
9. B. Choi, J. Lee, J. Yoon, J.-H. Ahn, T. J. Park, D. M. Kim, D. H. Kim, and S.-J. Choi, *IEEE Trans. Electron Devices* 62, 1072 (2015).
10. R. A. Chapman, P. G. Fernandes, H. J. Stiegler, H.-C. Wen, Y. J. Chabal, and E. M. Vogel, *IEEE Trans. Electron Devices* 58, 1752 (2011).
11. J. Lee, J. M. Lee, J. H. Lee, M. Uhm, W. H. Lee, S. Hwang, I. Y. Chung, B. G. Park, D. M. Kim, Y. J. Jeong, and D. H. Kim, *IEEE Electron Device Lett.* 34, 135 (2013).
12. J. Lee, J. M. Lee, J. H. Lee, W. H. Lee, M. Uhm, B. G. Park, D. M. Kim, Y. J. Jeong, and D. H. Kim, *IEEE Electron Device Lett.* 33, 1768 (2012).

Received: 18 August 2016. Accepted: 24 February 2017.